Identification of Myc-associated protein with JmjC domain as a novel therapeutic target oncogene for lung cancer

Chie Suzuki,[1] Koji Takahashi,[1] Satoshi Hayama,[1] Nobuhisa Ishikawa,[1] Tatsuya Kato,[1] Tomoo Ito,[2] Eiju Tsuchiya,[3] Yusuke Nakamura,[1] and Yataro Daigo[1]

[1]Laboratory of Molecular Medicine, Human Genome Center, Institute of Medical Science, The University of Tokyo, Tokyo, Japan; [2]Department of Surgical Pathology, Hokkaido University Graduate School of Medicine, Sapporo, Japan; and [3]Kanagawa Cancer Center Research Institute, Kanagawa, Japan

Abstract

Through genome-wide expression profile analysis for non–small cell lung cancers (NSCLC), we found overexpression of a Myc-associated protein with JmjC domain (*MAPJD*) gene in the great majority of NSCLC cases. Induction of exogenous expression of MAPJD into NIH3T3 cells conferred growth-promoting activity. Concordantly, *in vitro* suppression of MAPJD expression with small interfering RNA effectively suppressed growth of NSCLC cells, in which MAPJD was overexpressed. We found four candidate MAPJD target genes, *SBNO1, TGFBRAP1, RIOK1*, and *RASGEF1A*, which were the most significantly induced by exogenous MAPJD expression. Through interaction with MYC protein, MAPJD transactivates a set of genes, including kinases and cell signal transducers that are possibly related to proliferation of lung cancer cells. As our data imply that MAPJD is a novel member of the MYC transcriptional complex and its activation is a common feature of lung cancer, selective suppression of this pathway could be a promising therapeutic target for treatment of lung cancers. [Mol Cancer Ther 2007;6(2):542–51]

Introduction

Lung carcinoma is one of the most common causes of cancer death worldwide, and non–small cell lung cancer (NSCLC) accounts for ~80% of these cases (1). Although various cytotoxic agents offer multiple therapeutic choices for patients, each of the new regimens can provide only modest survival benefits to advanced NSCLC patients (2–4). Hence, development of novel therapeutic strategies, such as molecular targeted agents and antibodies as well as cancer vaccines, based on well-characterized molecular mechanisms involved in pulmonary carcinogenesis, are eagerly awaited.

Systematic analysis of expression levels of thousands of genes on a cDNA microarray is an effective approach to identify molecules involved in carcinogenic pathways (5–9); some of these genes or their products should be candidate targets for development of novel anticancer drugs and useful tumor markers. To isolate such molecules, we have been analyzing genome-wide expression profiles of lung cancers, using purified populations of tumor cells that were prepared by laser microbeam microdissection (5–9). To verify the biological and clinical significance of the respective gene products, we have established a screening system by a combination of the tumor tissue microarray analysis of clinical lung cancer materials as well as RNA interference (RNAi) technique (9–19). In the course of these systematic studies, we found Myc-associated protein with JmjC domain (MAPJD); C14orf169, chromosome 14 open reading frame 169; alias FLJ21802/NO66 protein to be overexpressed in the great majority of the NSCLCs. MAPJD was reported previously as a nuclear protein with a conserved JmjC domain that was commonly found in DNA- or chromatin-binding domains (20). JmjC domain-containing proteins are supposed to have the enzymatic activity that regulates chromatin remodeling and gene expressions. However, the role(s) of the members belonging to the JmjC-containing family in carcinogenic processes has not been clarified.

The *MYC* (*c-Myc*) oncogene is one of the most frequently overexpressed genes in human cancer (21). The expression level of *MYC* is tightly associated with cell proliferation in part by regulating genes involved in cell cycle control. MYC functions as a sequence-specific transcription factor belonging to the basic, helix-loop-helix, leucine zipper family. When dimerized with MYC-associated factor X, MYC binds to CACGTG (CANNTG) motifs (E-box) in the genome and activates the transcription of various target genes (22, 23). Recently, transcriptional activity of MYC/MYC-associated factor X heterodimers was linked to recruitment of cofactor complexes, including a transformation/transcription domain-associated protein (TRRAP) together with p300/CBP-associated factor (alias GCN5; ref. 24) or TIP60 histone acetyltransferases (HAT; ref. 25).

Here, we report that MAPJD plays a significant role in pulmonary carcinogenesis by activating various downstream target genes through interaction with MYC and suggest that this molecule represents a potential target for development of novel therapeutic drugs for lung cancer.

Received 10/25/06; revised 11/20/06; accepted 12/21/06.

The costs of publication of this article were defrayed in part by the payment of page charges. This article must therefore be hereby marked *advertisement* in accordance with 18 U.S.C. Section 1734 solely to indicate this fact.

Requests for reprints: Yataro Daigo, Laboratory of Molecular Medicine, Human Genome Center, Institute of Medical Science, The University of Tokyo, 4-6-1 Shirokanedai, Minato-Ward, Tokyo 108-8639, Japan. Phone: 81-3-5449-5457; Fax: 81-3-5449-5406. E-mail: ydaigo@ims.u-tokyo.ac.jp

doi:10.1158/1535-7163.MCT-06-0659

Materials and Methods

Cell Lines and Clinical Samples

The 30 human NSCLC cell lines used for this study were as follows: A427, A549, LC174, LC176, LC319, PC-3, PC-9, PC-14, SW900, SW1573, NCI-H23, NCI-H226, NCI-H358, NCI-H520, NCI-H522, NCI-H596, NCI-H647, NCI-H1373, NCI-H1435, NCI-H1650, NCI-H1666, NCI-H1703, NCI-H1781, NCI-H1793, NCI-H2170, RERF-LC-AI, SK-LU-1, SK-MES-1, EBC-1, and LX-1. All cells were grown in monolayer in appropriate medium supplemented with 10% FCS and maintained at 37°C in an atmosphere of humidified air with 5% CO_2. Human small airway epithelial cells and bronchial epithelial cells were also included in the panel of the cells used in this study. Primary NSCLC samples had been obtained earlier with informed consent (5).

A total of 300 formalin-fixed primary NSCLCs and adjacent normal lung tissue samples used for immunostaining on tissue microarrays had been obtained with informed consent from patients undergoing surgery earlier at Hokkaido University and its affiliated hospitals (Sapporo, Japan). The use of clinical materials in this study was approved by each of individual institutional ethical committees.

Semiquantitative Reverse Transcription-PCR

We prepared appropriate dilutions of each single-stranded cDNA prepared from mRNAs of clinical lung cancer samples and normal tissues (heart, liver, lung, bone marrow, testis, ovary, and placenta), using the level of β-actin (*ACTB*) expression as a quantitative control. The primer sets for amplification were as follows: *ACTB*-F (5′-GAGGTGATAGCATTGCTTTCG-3′) and *ACTB*-R (5′-CAAGTCAGTGTACAGGTAAGC-3′) for *ACTB*; *MAPJD*-F (5′-AGGAGAAGTTGGAGGTGGAAA-3′) and *MAPJD*-R (5′-CAGATGAAAGATCCAAATTCCAA-3′) for *MAPJD*; *SBNO*-F (5′-CTGACAGTGCATGTCTTTGG-3′) and *SBNO*-R (5′-TTCTGCAGCACACATTAGGA-3′) for sno, strawberry notch homologue 1 (*SBNO*; AK001563); *TGFBRAP1*-F (5′-GGGCTAACAATAAAGGCAGTC-3′) and *TGFBRAP1*-R (5′-CAACACATGGATGTTTTTGC-3′) for transforming growth factor-β receptor–associated protein 1 (*TGFBRAP1*; NM_004257); *RIOK1*-F (5′-GAAGACAGCCAAGACGAAAA-3′) and *RIOK1*-R (5′-TCCTCTGTCAACACCAGACA-3′) for RIO kinase 1 (*RIOK1*; yeast; NM_031480); and *RASGEF1A*-F (5′-TTTCCCATGTCTGACTTCGT-3′) and (5′-CAATGTCTTCAGGCTCTTCC-3′) for RasGEF domain family, member 1A (*RASGEF1A*; NM_145313). All reactions involved initial denaturation at 94°C for 2 min followed by 21 (for *ACTB*) or 30 (for others) cycles of 95°C for 30 s, 58°C to 62°C for 30 s, and 72°C for 45 s on a GeneAmp PCR system 9700 (Applied Biosystems, Foster City, CA).

Northern Blot Analysis

Human multiple-tissue blots (23 normal tissues, including brain, heart, skeletal muscle, colon, thymus, spleen, kidney, liver, small intestine, placenta, lung, peripheral blood leukocyte, adrenal gland, bladder, bone marrow, lymph node, prostate, spinal cord, stomach, thyroid, tongue, trachea, and uterus; BD Biosciences Clontech, Palo Alto, CA) were hybridized with a ^{32}P-labeled PCR product of *MAPJD*. The cDNA probe of *MAPJD* was synthesized by reverse transcription-PCR (RT-PCR) using a set of primers: *MAPJD*-F2 (5′-CTGGAAACAAGGCAGTAGTGATT-3′) and *MAPJD*-R2 (5′-GTACACTGAAGCCTGAAGGTGAT-3′). Prehybridization, hybridization, and washing were done according to the supplier's recommendations. The blots were autoradiographed with intensifying screens at room temperature for 14 days.

Western Blotting

Rabbit antibodies specific for MAPJD were raised by immunizing rabbits with recombinant human MAPJD protein and purified using standard protocols. Anti-myc antibody (9E10; Santa Cruz Biotechnology, Inc., Santa Cruz, CA) and anti-Flag antibody (M2; Santa Cruz Biotechnology) were used for detecting exogenously expressed proteins. We used an enhanced chemiluminescence Western blotting analysis system (GE Healthcare Biosciences, Piscataway, NJ). Cells were lysed in appropriate amounts of lysing buffer [150 mmol/L NaCl, 50 mmol/L Tris-HCl (pH 8.0), 1% NP40, 0.1% SDS, 0.5% sodium deoxycholate, plus protease inhibitor]. Proteins separated by SDS-PAGE were electroblotted onto nitrocellulose membranes (GE Healthcare Biosciences) and incubated with antibodies. A sheep anti-mouse IgG-horseradish peroxidase antibody (GE Healthcare Biosciences) and a goat anti-rabbit IgG-horseradish peroxidase antibody (GE Healthcare Biosciences) were served as the secondary antibodies for the experiments.

Immunohistochemistry and Tissue Microarray

Tumor tissue microarrays prepared from formalin-fixed lung cancers were constructed as published previously (26–28). The staining pattern of MAPJD was assessed semiquantitatively as absent or positive by three independent investigators without prior knowledge of the clinical follow-up data. Cases with <20% of nuclear MAPJD-stained tumor cells were judged as MAPJD negative. Cases were accepted as positive only if reviewers independently defined them as such. We confirmed that the antibody was specific to MAPJD, on Western blots using lysates from cell lines that had been transfected with MAPJD expression vector as well as by immunocytochemical staining of cell lines that either expressed MAPJD endogenously or not.

To investigate the presence of MAPJD protein in tissue microarrays of clinical samples, we stained the sections using EnVision+ Kit/horseradish peroxidase (DakoCytomation, Glostrup, Denmark). Rabbit antibody to human MAPJD was added after blocking endogenous peroxidase and proteins, and the tissue sections were incubated with horseradish peroxidase–labeled anti-rabbit IgG as the secondary antibody. Substrate chromogen was added and the specimens were counterstained with hematoxylin.

RNAi Assay

We had established a vector-based RNAi system, psiH1BX3.0, to direct the synthesis of small interfering RNAs (siRNA) in mammalian cells, as reported elsewhere (10, 12, 13, 15–19). Ten micrograms of aliquots of siRNA expression vector were transfected into NSCLC cell lines LC319 and A549, using 30 μL LipofectAMINE 2000 (Invitrogen, Carlsbad, CA). The transfected cells were cultured for 5 days in the presence of appropriate

concentrations of geneticin (G418). Viable cell numbers were measured by Giemsa staining and 3-(4,5-dimethylthiazol-2-yl)-2,5-diphenyltetrazolium bromide assays in triplicate. The target sequences of the synthetic oligonucleotides for RNAi were as follows: control (LUC: luciferase gene from *Photinus pyralis*), 5′-CGTACGCGGAATACTTCGA-3′; scramble (SCR: gene coding for 5 S and 16 S rRNAs in chloroplasts of *Euglena gracilis*), 5′-GCGCGCTTTGTAGGATTCG-3′; siRNA-*MAPJD*-1 (si-*MAPJD*-1: 5′-CGCAGCTGCGAAGTGTTGTA-3′); and siRNA-*MAPJD*-2 (si-*MAPJD*-2: 5′-GATACGAAAGCAGCTGCGA-3′). To validate our RNAi system, down-regulation of *MAPJD* expression by functional siRNAs, but not by controls, was also confirmed in the cell lines used for this assay.

Flow Cytometry

Cells were plated at densities of 5×10^5/100-mm dish, transfected with siRNA expression vectors, and cultured in the presence of appropriate concentrations of geneticin. Cells were trypsinized 5 days after the transfection, collected in PBS, and fixed in 70% cold ethanol for 30 min. After treatment with 100 μg/mL RNase (Sigma-Aldrich Co., St. Louis, MO), the cells were stained with 50 μg/mL propidium iodide (Sigma-Aldrich) in PBS. Flow cytometry was done on a Becton Dickinson FACScan and analyzed by ModFit software (Verity Software House, Inc., Topsham, ME). The cells selected from at least 20,000 ungated cells were analyzed for DNA content. Cells were also prepared using Annexin V-FITC Apoptosis Detection kit (BioVision, Inc., Mountain View, CA) for Annexin V binding assay according to the supplier's protocol.

MAPJD-Expressing NIH3T3 Transfectants

MAPJD-expressing stable transfectants were established according to a standard protocol. The entire coding region of MAPJD was amplified by RT-PCR using the primer sets MAPJD-F3 (5′-CCGGAATTCCGGGCCACCATGGATGGGCTCCAGGCCAGTGCAGG-3′) and MAPJD-R3 (5′-CCGCTCGAGCGGATTTAGGGCTAGAGGCATCTTAG-3′). The product was digested with *Eco*RI and *Xho*I and cloned into appropriate sites of a pcDNA3.1-myc/His A(+) vector (Invitrogen) that contained c-myc/His epitope sequences (LDEESILKQE-HHHHHH) at the COOH terminus of the MAPJD protein. Using Fugene 6 transfection reagent (Roche Diagnostics, Basel, Switzerland) according to the manufacturer's instructions, we transfected NIH3T3 cells, which do not express endogenous MAPJD, with plasmids expressing either MAPJD (pcDNA3.1-MAPJD-myc/His) or mock plasmids (pcDNA3.1). Transfected cells were cultured in DMEM containing 10% FCS and geneticin (0.4 mg/mL) for 14 days, and then, 50 individual colonies were trypsinized and screened for stable transfectants by a limiting dilution assay. Expression of MAPJD was determined in each clone by RT-PCR, Western blotting, and immunostaining. NIH3T3 transfectants that stably expressed MAPJD were seeded onto six-well plates (5×10^4 cells per well) and maintained in medium containing 10% FCS and 0.4 mg/mL geneticin for 24, 48, 72, and 96 h. At each time point, cell proliferation was evaluated by the 3-(4,5-dimethylthiazol-2-yl)-2,5-diphenyltetrazolium bromide assay in triplicate.

Identification of Downstream Genes of MAPJD by cDNA Microarray

LC319 cells were transfected with either siRNA against *MAPJD* (si-*MAPJD*-2) or luciferase (control siRNA). mRNAs were extracted 12, 18, and 24 h after the transfection, labeled with Cy5 or Cy3 dye, and subjected to cohybridization onto cDNA microarray slides containing 23,040 genes as described (17). After normalization of the data, genes with signals higher than the cutoff value were analyzed further. Genes whose intensity was significantly decreased in accordance with the reduction of *MAPJD* expression were initially selected using self-organizing map cluster analysis (29). Validation of candidate downstream genes of *MAPJD* was done with semiquantitative RT-PCR experiments of the same mRNAs from LC319 cells used for microarray hybridization, with gene-specific primers.

Reporter Gene Assay

The fragment of each downstream gene was amplified by PCR using the following primers: *SBNO*-F3 (5′-CGACGCGTCGCTCTAACCATTCATCAGCTC-3′) and *SBNO*-R2

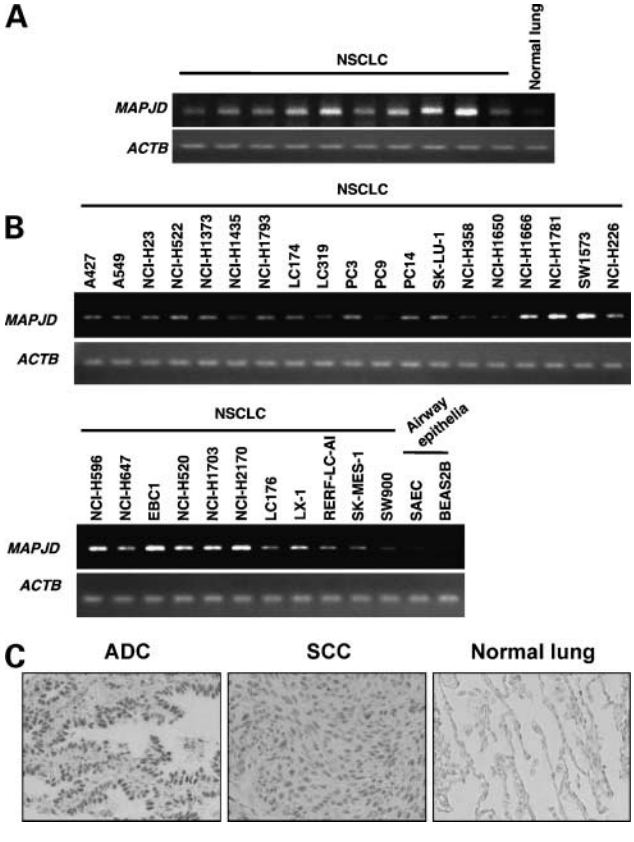

Figure 1. MAPJD expression in lung cancers. **A,** expression of *MAPJD* gene in clinical samples of NSCLC, examined by semiquantitative RT-PCR. We prepared appropriate dilutions of each single-stranded cDNA prepared from mRNAs of clinical lung cancer samples, monitoring the level of β-actin (*ACTB*) expression as a quantitative control. **B,** expression of *MAPJD* gene in lung cancer cell lines. *Top* and *bottom,* derived from a single gel. **C,** immunohistochemical evaluation of representative samples from surgically resected adenocarcinoma (*ADC*) and squamous cell carcinoma (*SCC*) tissues, using anti-MAPJD polyclonal antibody.

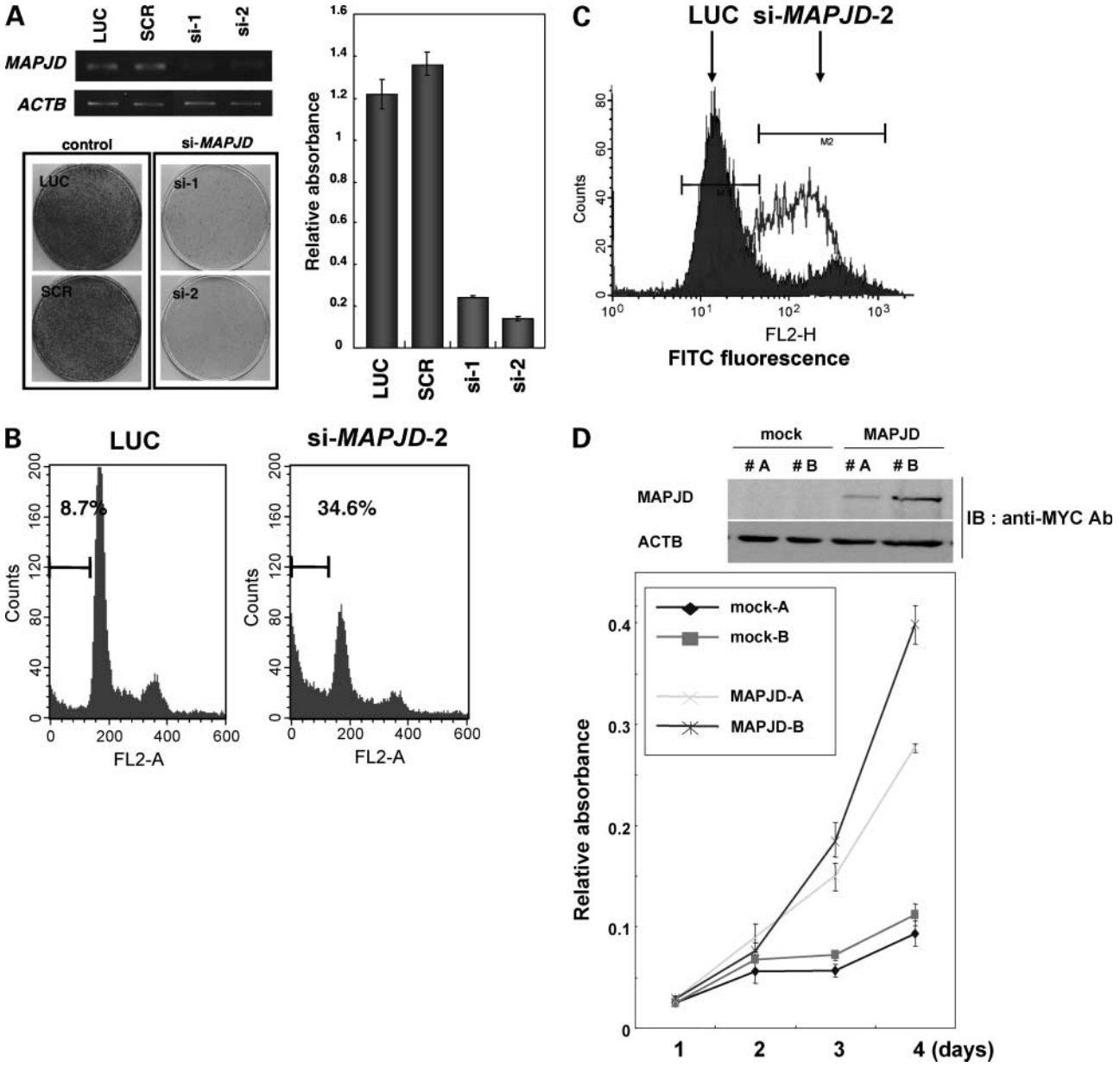

Figure 2. Effect of MAPJD on cell growth. **A** to **C,** growth inhibition of NSCLC cells by siRNA against *MAPJD*. **A,** expression of *MAPJD* in response to siRNA-*MAPJD*-1 (*si-1*), siRNA-*MAPJD*-2 (*si-2*), or control siRNAs against luciferase (*LUC*) or scramble (*SCR*) in LC319 cells, analyzed by semiquantitative RT-PCR (*left, top*). Colony formation assays of LC319 cells transfected with the specific siRNAs for MAPJD (*si-1* and *si-2*) or control plasmids (*left, bottom*). Viability of LC319 cells evaluated by 3-(4,5-dimethylthiazol-2-yl)-2,5-diphenyltetrazolium bromide assay in response to the siRNA-*MAPJDs* (*si-1* and *si-2*), in comparison with the two control siRNAs (*right*). Assays were done thrice in triplicate wells. *Y axis,* absorbance at 490 and at 630 nm as reference measured with a microplate reader. **B,** the sub-G_1 proportion of cells treated with control siRNA (*LUC*; *left*) or si-2 (*right*), detected by flow cytometric analysis. **C,** Annexin V binding assay using flow cytometric analysis of LC319 cells treated with control siRNA or si-2. The cells were labeled with Annexin V-FITC, fixed, and then analyzed by flow cytometry. *Black histogram,* the distribution of si-LUC–treated cells; *histogram with black line,* si-MAPJD–treated cells. Annexin V–negative cells were distributed in M1 region, whereas Annexin V–positive apoptotic cells were in M2 region. **D,** effect of MAPJD on growth of NIH3T3 cells. Expression of MAPJD-myc/His protein in stable transfectants of NIH3T3 cells on Western blots using anti-MYC antibody (*top*). Cell viability of the stable transfectants evaluated by the 3-(4,5-dimethylthiazol-2-yl)-2,5-diphenyltetrazolium bromide assay (*bottom*). Assays were done thrice in triplicate wells.

for *SBNO*; *TGFBRAP1*-F3 (5′-CGACGCGTCGAGACATTCTGACCATAGCACC-3′) and *TGFBRAP1*-R2 for *TGFBRAP1*; *RIOK1*-F3 (5′-CGACGCGTCGTTCCTACAATGTCTTCAGTC-3′) and *RIOK1*-R2 for *RIOK1*; and *RASGEF1A*-F3 (5′-CGACGCGTCGCAAGACCTTCACCATGTGG-3′) and *RASGEF1A*-R2 for *RASGEF1A*. The fragment of each downstream gene was also cloned into the pGL3 basic vector. Luciferase assays were done using

a Dual-Luciferase Reporter Assay System according to the manufacturer's instructions (Promega, Madison, WI).

Immunoprecipitation Assays

Lung cancer LC319 cells (5×10^6), transfected with plasmids expressing MAPJD or c-MYC (p3XFLAG-MAPJD or MYC), or the mock vector (control) were incubated in 1 mL lysis buffer (0.5% NP40, 50 mmol/L Tris-HCl, 150 mmol/L NaCl) in the presence of proteinase inhibitor. Cell extracts were precleared by incubation at 4°C for 1 h with 100 μL protein G-Agarose beads, in final volumes of 2 mL lysis buffer in the presence of proteinase inhibitor. Immunoprecipitation and additional Western blotting using antibodies specific for endogenous MAPJD, MYC (Santa Cruz Biotechnology), TRRAP (sc-11411), and TIP60 (sc-5725) were done as described elsewhere (12, 15, 18).

Chromatin Immunoprecipitation Assay

Cells were cross-linked in 1% formaldehyde for 10 min. The fixed chromatin samples were subjected to immunoprecipitation using chromatin immunoprecipitation (ChIP) assay kit according to the manufacturer's instructions (Upstate, Charlottesville, VA). The sets of primers used for ChIP assay are *SBNO*-F2 (5′-CGACGCGTCGTCTGTTCT-GAGCTTCCATAC-3′) and *SBNO*-R2 (5′-CCGCTCGAGCG-GACTAATTCCACTCTCAC-3′) for *SBNO*; *TGFBRAP1*-F2 (5′-CGACGCGTCGGAAAGTCTCACTTCCAATGG-3′) and *TGFBRAP1*-R2 (5′-CCGCTCGAGCGGATCATGTC-TACTGGCTGATC-3′) for *TGFBRAP1*; *RIOK1*-F2 (5′-CGACGCGTCGATAGATGTTCCAGAGACATTC-3′) and *RIOK1*-R2 (5′-CCGCTCGAGCGGTTCAGAAGCCAA-CAGTGGC-3′) for *RIOK1*; and *RASGEF1A*-F2 (5′-CGACGCGTCGCACTGAAGTAATCATGGCAAC-3′) and *RASGEF1A*-R2 (5′-CCGCTCGAGCGGAGACAACG-GACGTCTGCG-3′) for *RASGEF1A*.

Electrophoretic Mobility Shift Assay

Electrophoretic mobility shift assay was done by incubating immunoprecipitated or recombinant proteins (MAPJD or MYC) with ^{32}P-labeled oligonucleotide using a standard protocol. The sequences of oligonucleotides for the dsDNA probe were 5′-CCCGTCGCACGTGGTGGCCA-3′ and 5′-TGGCCACCACGTGCGACGGG-3′.

Results

Expression of MAPJD in Lung Cancers and Normal Tissues

We previously screened 27,648 genes on a cDNA microarray to screen transcripts that showed 3-fold or higher expression in cancer cells than in normal control cells in more than half of NSCLCs analyzed. Among the up-regulated genes, we identified the C14orf169 (later termed to *MAPJD*, due to evidences shown below) transcript and confirmed its increased expression in 9 of 10 representative NSCLC cases by semiquantitative RT-PCR experiments (Fig. 1A). We also observed high levels of *MAPJD* expression in 27 of the 30 lung cancer cell lines, whereas a very weak band of the PCR product was detectable in cells derived from normal airway epithelia (small airway epithelial cells and bronchial epithelial cells; Fig. 1B). Northern blotting using *MAPJD* cDNA as a probe identified a very weak 2.5-kb band ubiquitously in 23 normal human tissues examined, and additional semiquantitative RT-PCR experiments using the same primers as above detected *MAPJD* transcript in lung cancer cells, much more abundantly than normal tissues examined (heart, liver, lung, bone marrow, testis, ovary, and placenta; data not shown).

Immunohistochemical analysis with anti-MAPJD polyclonal antibody using tissue microarrays consisting of 300 NSCLCs revealed positive staining of the nucleus in 80% of adenocarcinomas (132 of 164 cases examined), 81% of squamous cell carcinomas (85 of 105 cases), 62% of large cell carcinomas (13 of 21 cases), and 90% of bronchioloalveolar cell carcinomas (9 of 10 cases), whereas, no detectable staining was observed in any of their adjacent normal lung tissues (Fig. 1C).

Effects of MAPJD on Cell Growth

To assess whether MAPJD is essential for growth or survival of lung cancer cells, we designed and constructed plasmids to express siRNA against *MAPJD* (si-*MAPJD*-1 and si-*MAPJD*-2) and two control siRNAs (for luciferase or scramble) and transfected each of them into LC319 and A549 cells (representative data of LC319 was shown in Fig. 2A). The amount of *MAPJD* transcript in the lung cancer cells transfected with each of si-*MAPJD*-1 and si-*MAPJD*-2 was significantly decreased in comparison with those transfected with either of the two control siRNAs (Fig. 2A, *left, top*); transfection of si-*MAPJD*-1 or si-*MAPJD*-2 also resulted in significant decreases in colony numbers and cell viability measured by colony formation and 3-(4,5-dimethylthiazol-2-yl)-2,5-diphenyltetrazolium bromide assays (si-2 versus luciferase, $P = 1.1 \times 10^{-7}$, unpaired t test; Fig. 2A, *left, bottom*; *right*). To clarify the mechanisms of this phenotype further, we did flow cytometrical analysis using LC319 cells that had been transfected with si-*MAPJD*-2 and found that the sub-G_1 proportion of cells treated with si-*MAPJD*-2 was significantly higher than those treated with control siRNA against *LUC* (Fig. 2B). Moreover, we confirmed increased number of apoptotic cells transfected with si-*MAPJD*-2 compared with those transfected with luciferase using Annexin V binding assay (Fig. 2C).

To further verify a potential role of MAPJD in tumorigenesis, we established NIH3T3 cells that stably expressed exogenous MAPJD. The growth rate of NIH3T3-derivative cells that stably expressed MAPJD was much higher than that of cells transfected with mock plasmid in a MAPJD dose-dependent manner (Fig. 2D).

Identification of MAPJD Target Genes

Because MAPJD was present in nucleus and includes a JmjC domain, which is suggested to play an important role in the transcriptional regulation, we first attempted to identify downstream genes specifically regulated by MAPJD in cancer cells. siRNA-*MAPJD*-2 or siRNA-LUC (control siRNA) was transfected into LC319 cells, in which MAPJD was expressed at a high level, and alterations in gene expression at various time points were monitored using a cDNA microarray consisting of 23,040 genes.

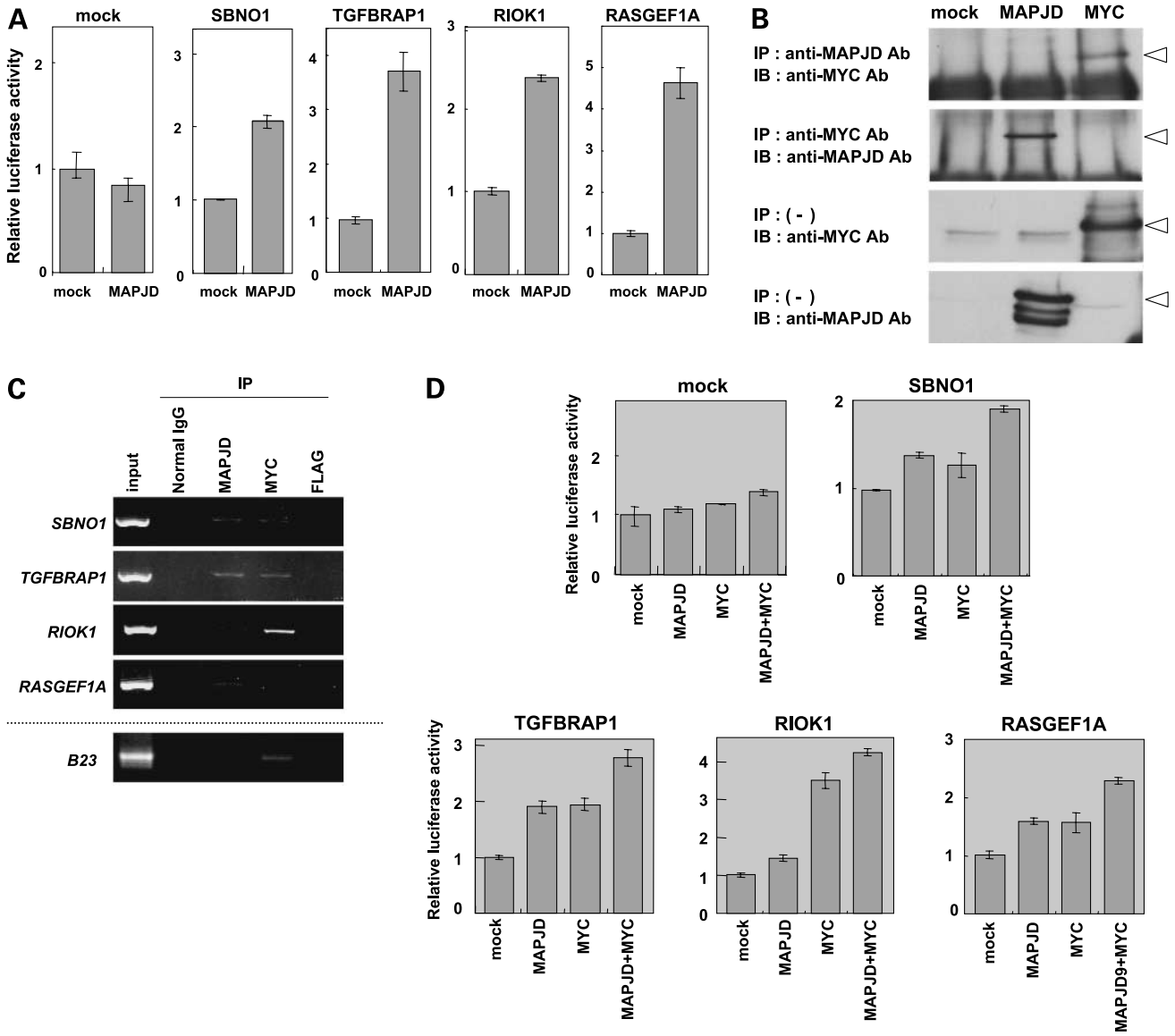

Figure 3. Identification of candidate downstream genes of MAPJD and interaction of MAPJD with MYC oncogene and their transcriptional regulation. **A,** effect of MAPJD on the luciferase activity of reporter plasmids containing the promoter region of each of the four candidate target genes in LC319 cells. *Y axis,* relative luciferase activity (luciferase values detected in cells expressing either MAPJD or MYC, or both, compared with those transfected with mock control). **B,** association of MAPJD and MYC. Reciprocal immunoprecipitation (*IP*) followed by immunoblotting (*IB*) with antibodies specific for MAPJD or MYC, using extracts of LC319 cells transfected with MAPJD or MYC expression vectors. **C,** association of endogenous MAPJD or MYC with DNA fragments containing a 1 kb upstream region of the putative transcription start sequence of the four candidate MAPJD target genes and *B23* gene (control for immunoprecipitation by representing the binding of MYC; see ref. 41), detected by ChIP assay. DNA from LC319 cells was immunoprecipitated with indicated antibodies and served for PCR. **D,** effect of exogenous MAPJD and MYC on the luciferase activity of LC319 cells transfected with reporter genes containing the promoter region of each MAPJD target gene.

Among hundreds of genes that had been down-regulated by this approach, we selected 53 genes whose expression were significantly decreased in accordance with the reduction of *MAPJD* expression by doing the self-organizing map clustering analysis (29). Semiquantitative RT-PCR analysis confirmed time-dependent reduction of these 53 candidate transcripts in LC319 cells transfected with si-*MAPJD*-2 (data not shown). We also evaluated the transactivation of these genes in accordance with introduction of exogenous *MAPJD* expression in lung cancer cell lines (data not shown) and finally selected four top candidate MAPJD target genes, *SBNO, TGFBRAP1, RIOK1*, and *RASGEF1A*, which were the most significantly induced by MAPJD expression.

To examine the possible promoter-specific transactivation of these target genes by MAPJD, we cotransfected into LC319 cells reporter plasmids containing a 1 kb upstream region of the putative transcription start site of each of the four genes

fused to a luciferase reporter gene and MAPJD-expressing plasmids. MAPJD-transfected cells displayed higher luciferase activity than mock-transfected cells (Fig. 3A).

Interaction of MAPJD with MYC and Their Transcriptional Regulation

The reporter gene assay suggested that MAPJD could act as a transcription factor or regulate gene expressions together with some transcription factor(s). Hence, we searched for candidate consensus binding motif of transcription factors common to regulatory regions of these four candidate MAPJD target genes and found that all of the four candidate genes contained several copies of E-box (CANNTG) in their possible transcriptional regulatory regions. Because MYC is one of the proteins binding to the E-box, we then examined and confirmed by immunoprecipitation assay an association of exogenously expressed MAPJD or MYC with endogenous ones in LC319 cells (Fig. 3B). To examine the association of MAPJD and/or MYC with promoter sites of the four genes, we did ChIP assay with anti-MAPJD antibody or anti-MYC antibodies using extracts of LC319 cells. Genomic segments corresponding to the 1 kb upstream region containing the putative transcription start sites were confirmed to be associated with both MAPJD and MYC proteins (Fig. 3C). To further confirm transcriptional activity of MAPJD and MYC on the MAPJD target genes, we did luciferase assay. LC319 cells transfected with MYC or MAPJD induced higher luciferase activity than those transfected with mock vector, indicating that MAPJD and MYC are responsible for the transactivation of these four genes (Fig. 3D). Moreover, cotransfection of both MAPJD and MYC expression plasmids further increased luciferase activity of reporter

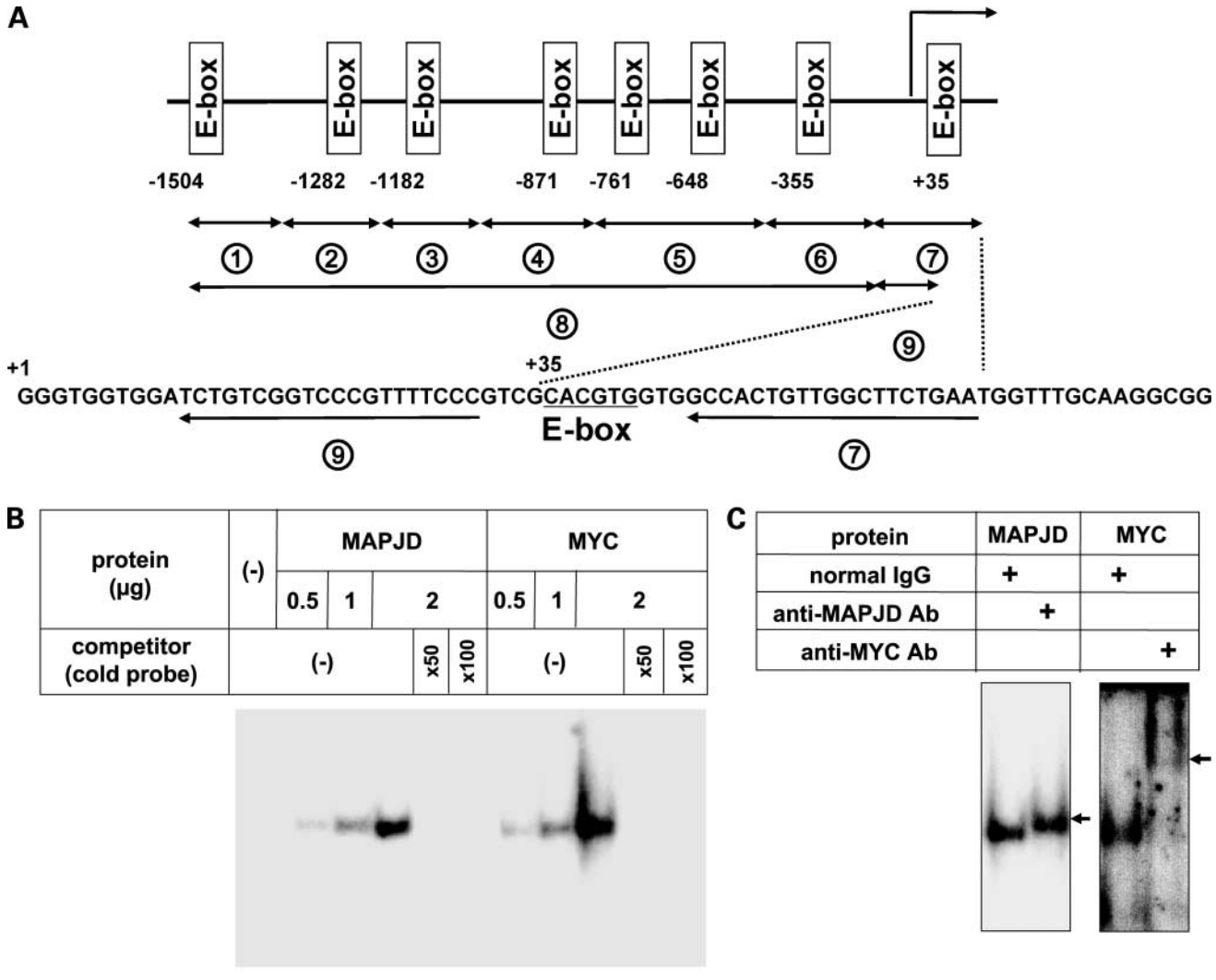

Figure 4. Interaction of MAPJD with E-box sequence of the *RIOK1* gene. **A,** positions of E-box motifs in the 5′ flanking region of the *RIOK1* gene. **B** and **C,** sequence-specific binding of MAPJD to E-box motif, detected by EMSA. MAPJD or MYC protein was incubated with a DNA probe containing the E-box sequence in the genomic segment-7, with or without a competitor (**B**), as well as with or without anti-MAPJD or MYC antibody (**C**). *Arrowheads,* supershifted bands.

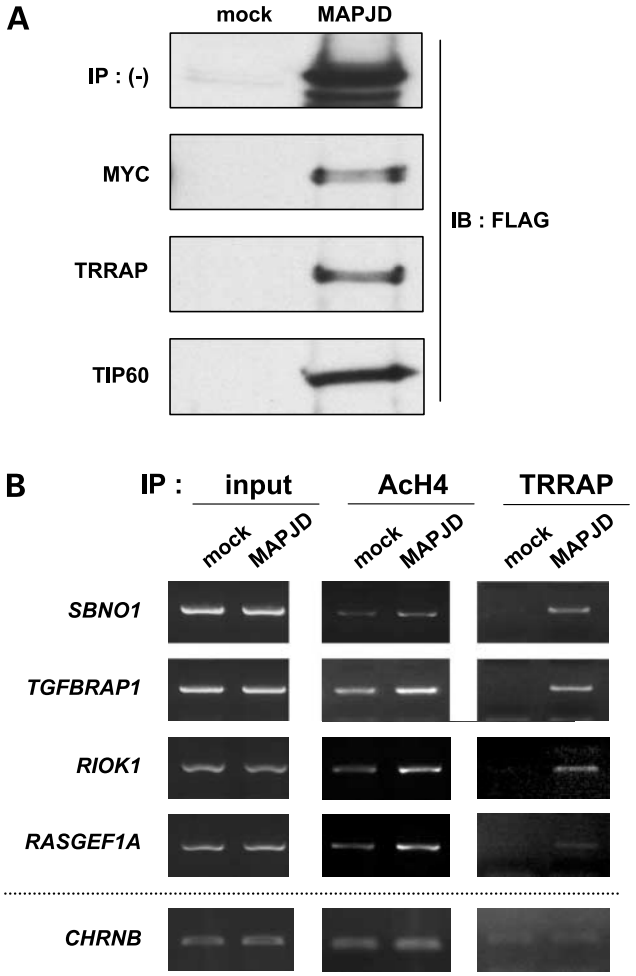

Figure 5. Enhancement of MYC-related HAT complex recruitment to the target genes and histone H4 acetylation by MAPJD. **A,** interaction of MAPJD with HAT complex containing MYC. Immunoprecipitation with antibodies to endogenous MYC, TRRAP, or TIP60 followed by immunoblotting with anti-FLAG antibody (M2), using extracts of LC319 cells transfected with FLAG-MAPJD – expressing or mock vectors. **B,** association of acetylated histone H4 (*AcH4*) and endogenous TRRAP with DNA fragments of 5′-flanking region containing E-boxes of the four MAPJD target genes, *SBNO1, TGFBRAP1, RIOK1*, and *RASGEF1A*, detected by ChIP assay. DNAs from LC319 cells transfected with MAPJD-expressing or mock vectors were immunoprecipitated with indicated antibodies and served for PCR. CHRNB (cholinergic receptor, nicotinic, β1, and muscle; see ref. 41) was used as a quantitative control.

plasmids (Fig. 3D). These data suggest that MAPJD and MYC could form a complex and synergistically regulate the transcriptional activity of the candidate MAPJD target genes.

We subsequently focused on the E-box motifs in the possible promoter region of the *RIOK1* gene, which has eight E-box motifs from −1504 to +35 (Fig. 4A). ChIP assay with anti-MAPJD and anti-MYC antibodies using nuclear extracts of LC319 cells detected that only the genomic segment-7 containing an E-box motif seemed to be most significantly associated with endogenous MAPJD, whereas MYC almost equally bound to all of the seven segments (data not shown). These data suggest that MAPJD was possibly associated with the E-box of segment-7 in the *RIOK1* gene. We also did an electrophoretic mobility shift assay using a double-stranded oligonucleotide probe that corresponds to the possible binding sequence and myc-tagged MAPJD protein purified by immunoprecipitation. A shifted band was detected in the presence of MAPJD, whereas no shifted band was observed after cold competitive oligonucleotides were added, supporting the specific interaction between the oligonucleotide probe and MAPJD (Fig. 4B, *left*). The band was supershifted after the addition of anti-MAPJD antibody, but not that of normal rabbit IgG, thus independently confirming the specific interaction (Fig. 4C, *left*). MYC also interacted with this probe specifically (Fig. 4B and C, *right*).

MAPJD Recruits MYC-Related HAT Complex to Regulatory Regions of Its Target Genes

MYC is known to activate gene transcription through binding to E-boxes in regulatory regions of its target genes and subsequent recruiting of a protein complex, including the TRRAP protein together with GCN5/p300/CBP-associated factor or TIP60 HATs that preferentially acetylate histones H3 and H4 (24, 25). Therefore, we investigated whether MAPJD could recruit the MYC-regulated HAT complex to the four MAPJD target genes (*SBNO1, TGFBRAP1, RIOK1*, and *RASGEF1A*) and increase the level of histone acetylation. We first confirmed by immunoprecipitation assay a cognate association of FLAG-tagged MAPJD with endogenous MYC-HAT complex proteins (TRRAP and TIP60) as well as endogenous MYC in LC319 cells (Fig. 5A). We then did ChIP assay with antibodies to TRRAP and triacetylated histone H4 using nuclear extracts of LC319 cells transfected with the MAPJD expression vector. We observed enhancement of the association

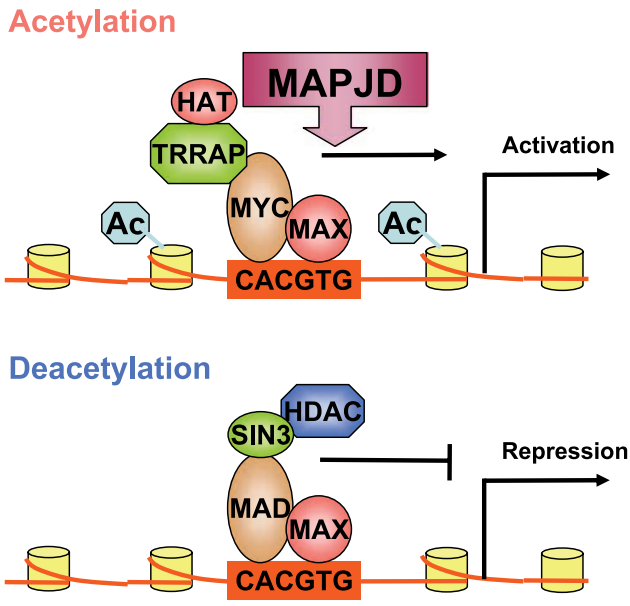

Figure 6. Schematic model for the mechanism of histone acetylation by MYC-related HAT complex and MAPJD. MAPJD-MYC complex might bind to the E-box site and recruit chromatin-modifying factors to this site.

between TRRAP and each of the gene regulatory regions as well as the increase in triacetylated histone H4 levels in the cells transfected with MAPJD expression plasmid (Fig. 5B). Although the precise mechanism should be further investigated, these data suggest that the MAPJD-MYC complex might bind to the E-box site and recruit chromatin-modifying factors to this site, as similar to an example of MYC/MYC-associated factor X (Fig. 6; refs. 23, 30).

Discussion

Molecular targeted drugs are expected to be highly specific to malignant cells and have minimal adverse reactions due to their well-defined mechanisms of action. Toward identification of appropriate molecular targets for development of such drugs, we combined genome-wide expression analysis for selecting genes that were overexpressed in lung cancer cells with high-throughput screening of loss-of-function effects by means of the RNAi technique (5–19). Using this systematic approach, we found MAPJD to be overexpressed commonly in clinical NSCLC samples as well as lung cancer cell lines and showed that overexpression of this gene product plays an indispensable role in the growth of lung cancer cells. MAPJD was initially identified in *Xenopus* as a dual location protein in the nucleolus and in a special type of synchronously replicating chromatin (20). The human *MAPJD* encodes a 641-amino acid protein with a JmjC domain. JmjC domain was found commonly in proteins bound to DNA or chromatin, and JmjC domain-containing proteins are thought to regulate chromatin structure and/or gene expressions by regulating modification of histones (20).

Many studies have shown that cell cycle progression rates are closely related to MYC levels (21). Modest increase in the levels of MYC was supposed to be an initiating event in the various forms of human cancer (21). MYC regulates the transcription of downstream target genes by recruiting the acetyltransferase complexes to the target genes. In this process, it was suggested that MYC may work through the modification of HAT activities, in concert with other chromatin remodeling enzymes, some of which may not be identified yet, and that different combinations of HATs and chromatin remodeling factors might be applied in different cellular conditions (21–25). We here showed that MAPJD transactivated a set of genes possibly related to lung cancer cell proliferation, by interacting with MYC. We identified four candidate downstream genes of MAPJD, *SBNO1, TGFBRAP1, RIOK1*, and *RASGEF1A*. Our data obtained by the reporter gene and ChIP assays using the E-box motifs in the possible promoter region of each of the four genes suggested that MYC and MAPJD might synergistically have the transactivating activity through their association with promoter sites of the target genes. Importantly, it should be noted that *TGFBRAP1* has only one E-box in the predicted promoter region examined (70 bp upstream of the transcription initiation site). This independently supports our hypothesis that MYC and MAPJD could synergistically bind to the same promoter and activate transcription of downstream genes, although future detailed studies with mutant promoter constructs could be required to clarify this mechanism. Interestingly, all of the four candidate MAPJD target genes have been supposed to be involved in oncogenic signalings. SBNO1 is a downstream component of the Notch signaling pathway that is known to function in the oncogenic process and is required during embryogenesis and oogenesis in *Drosophila* (31, 32). TGFBRAP1 binds to TGFB receptors that were reported to be related to tumorigenesis (33, 34). RIOK1 is overexpressed in colon cancers (35). RASGEF1A contains a RasGEF domain, which might play an important role in the Ras signaling pathway. Although, the precise function of these downstream genes in human carcinogenesis and even their physiologic function in mammalian cells remain to be elucidated, our data suggest that MAPJD could be one of the key regulators to selectively activate the transcription of several genes through the recruitment of HAT complex to chromatin and subsequent histone acetylation, along with MYC oncoprotein.

We confirmed that MAPJD localized at nucleolus and nucleoplasm in cancer cells (data not shown). The nucleolus is known to function in ribosome biogenesis, a complicated process that includes the transcription of rRNA genes, the processing and modification of these transcripts, and their assembly with both ribosomal proteins as well as nonribosomal ones to guide the formation of preribosomal particles (36, 37). In addition, it was reported recently that nucleolus also harbors diverse functions that involved the assembly of various other ribonucleoprotein particles, the modification of small RNAs, the control of the cell cycle, the sequestration of regulatory molecules, and nuclear export process (38, 39). It was reported recently that MYC bound to human rDNA in nucleoli and stimulated transcription of rRNA by associating with the RNA polymerase I–specific factor SL1 (40). The combined evidence suggests that MAPJD might also play an important role at nucleolus in cancer cells, by interacting with other nucleolar proteins as well as MYC.

In summary, we showed that MAPJD is involved in the gene transcription as a possible member of the MYC transcriptional complex. Because MAPJD is likely to be essential for promotion of growth of lung cancer, we suggest that it could be a novel therapeutic target for development of anticancer drugs.

References

1. Greenlee RT, Hill-Harmon MB, Murray T, Thun M. Cancer statistics. CA Cancer J Clin 2001;51:15 – 36.

2. Sozzi G. Molecular biology of lung cancer. Eur J Cancer 2001;37:63 – 73.

3. Kelly K, Crowley J, Bunn PA, Jr., et al. Randomized phase III trial of paclitaxel plus carboplatin versus vinorelbine plus cisplatin in the treatment of patients with advanced non-small-cell lung cancer: a Southwest Oncology Group trial. J Clin Oncol 2001;19:3210 – 8.

4. Schiller JH, Harrington D, Belani CP, et al. Eastern Cooperative Oncology Group. Comparison of four chemotherapy regimens for advanced non-small-cell lung cancer. N Engl J Med 2002;346:92 – 8.

5. Kikuchi T, Daigo Y, Katagiri T, et al. Expression profiles of non-small cell lung cancers on cDNA microarrays: identification of genes for prediction of lymph-node metastasis and sensitivity to anti-cancer drugs. Oncogene 2003;22:2192 – 205.

6. Kakiuchi S, Daigo Y, Tsunoda T, Yano S, Sone S, Nakamura Y. Genome-wide analysis of organ-preferential metastasis of human small cell lung cancer in mice. Mol Cancer Res 2003;1:485 – 99.

7. Kakiuchi S, Daigo Y, Ishikawa N, et al. Prediction of sensitivity of advanced non-small cell lung cancers to gefitinib (Iressa, ZD1839). Hum Mol Genet 2004;13:3029 – 43.

8. Kikuchi T, Daigo Y, Ishikawa N, et al. Expression profiles of metastatic brain tumor from lung adenocarcinomas on cDNA microarray. Int J Oncol 2006;28:799 – 805.

9. Taniwaki M, Daigo Y, Ishikawa N, et al. Gene expression profiles of small-cell lung cancers: molecular signatures of lung cancer. Int J Oncol 2006;29:567 – 75.

10. Suzuki C, Daigo Y, Kikuchi T, Katagiri T, Nakamura Y. Identification of COX17 as a therapeutic target for non-small cell lung cancer. Cancer Res 2003;63:7038 – 41.

11. Ishikawa N, Daigo Y, Yasui W, et al. ADAM8 as a novel serological and histochemical marker for lung cancer. Clin Cancer Res 2004;10:8363 – 70.

12. Kato T, Daigo Y, Hayama S, et al. A novel human tRNA-dihydrouridine synthase involved in pulmonary carcinogenesis. Cancer Res 2005;65: 5638 – 46.

13. Furukawa C, Daigo Y, Ishikawa N, et al. PKP3 oncogene as prognostic marker and therapeutic target for lung cancer. Cancer Res 2005;65: 7102 – 10.

14. Ishikawa N, Daigo Y, Takano A, et al. Increases of amphiregulin and transforming growth factor-α in serum as predictors of poor response to gefitinib among patients with advanced non-small cell lung cancers. Cancer Res 2005;65:9176 – 84.

15. Suzuki C, Daigo Y, Ishikawa N, et al. ANLN plays a critical role in human lung carcinogenesis through activation of RHOA and by involvement in PI3K/AKT pathway. Cancer Res 2005;65:11314 – 25.

16. Ishikawa N, Daigo Y, Takano A, et al. Characterization of SEZ6L2 cell-surface protein as a novel prognostic marker for lung cancer. Cancer Sci 2006;97:737 – 45.

17. Takahashi K, Furukawa C, Takano A, et al. The NMU-GHSR1b/NTSR1 oncogenic signaling pathway as a therapeutic target for lung cancer. Cancer Res 2006;66:9408 – 19.

18. Hayama S, Daigo Y, Kato T, et al. Activation of CDCA1-KNTC2, members of centromere protein complex, involved in pulmonary carcinogenesis. Cancer Res 2006;66:10339 – 48.

19. Kato T, Hayama S, Yamabuki Y, et al. Increased expression of IGF-II mRNA-binding protein 1 is associated with the tumor progression in patients with lung cancer. Clin Cancer Res. In press 2007.

20. Eilbracht J, Reichenzeller M, Hergt M, et al. NO66, a highly conserved dual location protein in the nucleolus and in a special type of synchronously replicating chromatin. Mol Biol Cell 2004;15:1816 – 32.

21. Nesbit CE, Tersak JM, Prochownik EV. Myc oncogenes and human neoplastic disease. Oncogene 1999;18:3004 – 16.

22. Blackwell TK, Kretzner L, Blackwood EM, Eisenman RN, Weintraub H. Sequence-specific DNA binding by the c-Myc protein. Science 1999;250: 1149 – 51.

23. Blackwood EM, Eisenman RN. Max: a helix-loop-helix zipper protein that forms a sequence-specific DNA-binding complex with Myc. Science 1991;251:1211 – 7.

24. McMahon SB, Wood MA, Cole MD. The essential cofactor TRRAP recruits the histone acetyltransferase hGCN5 to c-Myc. Mol Cell 2000;20: 556 – 62.

25. Frank SR, Parisi T, Taubert S, et al. Myc recruits the TIP60 histone acetyltransferase complex to chromatin. EMBO Rep 2003;4:575 – 80.

26. Chin SF, Daigo Y, Huang HE, et al. A simple and reliable pretreatment protocol facilitates fluorescent *in situ* hybridisation on tissue microarrays of paraffin wax embedded tumour samples. Mol Pathol 2003;56:275 – 9.

27. Callagy G, Cattaneo E, Daigo Y, et al. Molecular classification of breast carcinomas using tissue microarrays. Diagn Mol Pathol 2003;12: 27 – 34.

28. Callagy G, Pharoah P, Chin SF, et al. Identification and validation of prognostic markers in breast cancer with the complementary use of array-CGH and tissue microarrays. J Pathol 2005;205:388 – 96.

29. Kohonen T. The self-organizing map. IEEE 1990;78:1464 – 80.

30. Eisenman RN. Deconstructing Myc. Genes Dev 2001;15:2023 – 30.

31. Coyle-Thompson CA, Banerjee U. The *strawberry notch* gene functions with *Notch* in common developmental pathways. Development 1993;119:377 – 95.

32. Radtke F, Raj K. The role of Notch in tumorigenesis: oncogene or tumour suppressor? Nat Rev Cancer 2003;10:756 – 67.

33. Charng MJ, Zhang D, Kinnunen P, Schneider MD. A novel protein distinguishes between quiescent and activated forms of the type I transforming growth factor b receptor. J Biol Chem 1998;273:9365 – 8.

34. Wurthner JU, Frank DB, Felici A, et al. Transforming growth factor-β receptor associated protein 1 is a Smad4 chaperone. J Biol Chem 2001; 276:19495 – 502.

35. Line A, Slucka Z, Stengrevics A, Silina K, Li G, Rees RC. Characterization of tumour-associated antigens in colon cancer. Cancer Immunol Immunother 2002;51:574 – 82.

36. Scheer U, Hook R. Structure and function of the nucleolus. Curr Opin Cell Biol 1999;11:385 – 90.

37. Zao J, Yuan X, Frodin M, Grummt I. ERK-dependent phosphorylation of the transcription initiation factor TIF-IA is required for RNA polymerase I transcription and cell growth. Mol Cell 2003;11:405 – 13.

38. Olson MO, Hingorani K, Szebemi A. Conventional and nonconventional roles of the nucleolus. Int Rev Cytol 2002;219:199 – 266.

39. Gerbi SA, Borovjagin AV, Lange TS. The nucleolus: a site of ribonucleoprotein maturation. Curr Opin Cell Biol 2003;15:318 – 25.

40. Grandori C, Gomez-Roman N, Felton-Edkins ZA, et al. c-Myc binds to human ribosomal DNA and stimulates transactivation of rRNA genes by RNA polymerase I. Nat Cell Biol 2005;7:311 – 8.

41. Zeller KI, Haggerty TJ, Barrett JF, et al. Characterization of nucleophosmin (B23) as a Myc target by scanning chromatin immunoprecipitation. J Biol Chem 2001;276:48285 – 91.